THE JOURNAL OF BIOLOGICAL CHEMISTRY VOL. 281, NO. 31, pp. 21781–21788, August 4, 2006
Printed in the U.S.A.

An Interaction Involving an Arginine Residue in the Cytoplasmic Domain of the 5-HT_{3A} Receptor Contributes to Receptor Desensitization Mechanism*

Received for publication, January 23, 2006, and in revised form, May 25, 2006 Published, JBC Papers in Press, June 5, 2006, DOI 10.1074/jbc.M600676200

Xiang-Qun Hu[‡], Hui Sun[‡], Robert W. Peoples[§], Ren Hong[§], and Li Zhang[‡1]

From the [‡]Laboratory for Integrative Neuroscience, National Institute on Alcohol Abuse and Alcoholism, Bethesda, Maryland 20892-8115 and the [§]Department of Biomedical Sciences, College of Health Sciences, Marquette University, Milwaukee, Wisconsin 53201-1881

A large cytoplasmic domain accounts for approximately one-third of the entire protein of one superfamily of ligand-gated membrane ion channels, which includes nicotinic acetylcholine (nACh), γ-aminobutyric acid type A ($GABA_A$), serotonin type 3 (5-HT_3), and glycine receptors. Desensitization is one functional feature shared by these receptors. Because most molecular studies of receptor desensitization have focused on the agonist binding and channel pore domains, relatively little is known about the role of the large cytoplasmic domain (LCD) in this process. To address this issue, we sequentially deleted segments of the LCD of the 5-HT_{3A} receptor and examined the function of the mutant receptors. Deletion of a small segment that contains three amino acid residues (425–427) significantly slowed the desensitization kinetics of the 5-HT_{3A} receptor. Both deletion and point mutation of arginine 427 altered desensitization kinetics in a manner similar to that of the (425–427) deletion without significantly changing the apparent agonist affinity. The extent of receptor desensitization was positively correlated with the polarity of the amino acid residue at 427: the desensitization accelerates with increasing polarity. Whereas the R427L mutation produced the slowest desensitization, it did not significantly alter single channel conductance of 5-HT_{3A} receptor. Thus, the arginine 427 residue in the LCD contributes to 5-HT_{3A} receptor desensitization, possibly through forming an electrostatic interaction with its neighboring residues. Because the polarity of the amino acid residue at 427 is highly conserved, such a desensitization mechanism may occur in other members of the Cys-loop family of ligand-gated ion channels.

The Cys-loop pentameric ligand-gated ion channel (LGIC)[2] superfamily includes nicotinic acetylcholine (nACh), γ-aminobutyric acid type A ($GABA_A$), glycine, and serotonin type 3 (5-HT_3) receptors (1). These receptors play crucial roles in fast synaptic transmission through agonist-induced opening of transmembrane ion channels in the central and peripheral nervous systems. Topologically, these receptors consist of a large extracellular N-terminal domain, a large cytoplasmic domain (LCD), and four transmembrane domains (1). The 5-HT_3 receptor can modulate the release of neurotransmitters such as glutamate, GABA, and dopamine (DA), and plays a role in the reward mechanisms of drug addiction (2, 3). Of all five 5-HT_3 subunits identified by molecular cloning, the 5-HT_{3A} and 5-HT_{3B} subunits have been the most thoroughly characterized (4). Although the 5-HT_{3B} subunit can form a functional heteromer when co-expressed with the 5-HT_{3A} subunit (5), the 5-HT_{3A} subunit is capable of forming a functional channel (1), and such a homomer is thought to be the dominant functional form in the central nervous system (6).

One common feature shared by members of the LGIC superfamily is that these receptors desensitize at synaptic sites when exposure to agonist is prolonged. Desensitization plays a critical role in the regulation of neuronal excitability and the efficacy of synaptic transmission (7, 8). Several inherited mutations occurring in ACh receptors have been shown to alter receptor desensitization kinetics (9, 10). These mutations increase or decrease the synaptic response to ACh and result in slow or fast channel syndromes, which is thought to contribute to pathological mechanisms of certain types of neurological diseases (9–11). Like other members of the LGIC superfamily, 5-HT_3 receptors desensitize in the continued presence of agonist (12).

Mechanisms underlying receptor desensitization have been the focus of much research and discussions for the last several decades (7, 8). Despite extensive investigation, the molecular mechanisms of receptor desensitization are not totally understood. There are many factors that contribute to this physiological process. Desensitization kinetics may be affected by external calcium concentration (13), posttranslational modification of the receptor protein (14) and subunit composition (15). Both the large extracellular N-terminal domain and transmembrane domains of LGICs have been found to be important in regulation of receptor desensitization (16). Whereas recent studies have revealed the important involvement of the LCD of 5-HT_{3A} receptor in regulation of channel conductance and Ca^{2+} permeability (17), little is known about the structural and functional role of the LCD in receptor desensitization. To address this question, we sequentially deleted segments of the LCD in the 5-HT_{3A} receptor and expressed the mutant receptors in

* The costs of publication of this article were defrayed in part by the payment of page charges. This article must therefore be hereby marked "*advertisement*" in accordance with 18 U.S.C. Section 1734 solely to indicate this fact.

[1] To whom correspondence should be addressed: Laboratory for Integrative Neuroscience, NIAAA, National Institutes of Health, 5625 Fishers Lane, Bethesda, MD 20892-8115. Tel.: 301-443-3755; Fax: 301-480-0466; E-mail: lzhang@mail.nih.gov.

[2] The abbreviations used are: LGIC, ligand-gated ion channel; 5-HT, serotonin; ACh, acetylcholine; WT, wild type; LY, LY 278,584, LCD, large cytoplasmic domain; ANOVA, analysis of variance; PBS, phosphate-buffered saline; pS, picosiemens.

human embryonic kidney (HEK293) cells. The desensitization kinetics of these receptors was measured using a fast perfusion system. We identified a single arginine residue at 427 that is critical for 5-HT$_{3A}$ receptor desensitization kinetics. Deletion or point mutation of this residue substantially slowed receptor desensitization without significantly affecting agonist binding affinity. The magnitude of receptor desensitization is correlated with the polarity of the residue at 427. These findings suggest that the residue at 427 regulates 5-HT$_{3A}$ receptor desensitization by a hydrogen-bonding or ionic interaction with its neighboring amino acid residues. This structural element could play an important role in the conformational transition required for the desensitization of the 5-HT$_{3A}$ receptor as well as other members of the Cys-loop LGIC superfamily.

MATERIALS AND METHODS

Deletional Mutation and Site-directed Mutagenesis—Deletions and point mutations of the long isoform of the mouse 5-HT$_{3A}$ receptor were introduced using the QuikChange site-directed mutagenesis kit (Stratagene). The authenticity of the DNA fragments that flank the mutation site was confirmed by double-strand DNA sequencing using an ABI Prism 377 Automatic DNA Sequencer (Applied Biosystems).

Preparation of cRNAs and Expression of Receptors—Complementary RNAs (cRNAs) were synthesized *in vitro* from linearized template cDNAs with a mMACHINE RNA transcription kit (Ambion). The quality and the sizes of synthesized cRNAs were confirmed by denatured RNA-agarose gels. Mature female *Xenopus laevis* frogs were anesthetized by submersion in 0.2% 3-aminobenzoic acid ethyl ester (Sigma), and a group of oocytes was surgically excised. The oocytes were separated and the follicular cell layer was removed by treatment with type I collagenase (Roche Molecular Biochemicals) for 2 h at room temperature. Each oocyte was injected with a total of 20 ng of RNA in 20 nl of diethylpyrocarbonate-treated water and was incubated at 19 °C in modified Barth's solution (MBS: 88 mM NaCl, 1 mM KCl, 2.4 mM $NaHCO_3$, 2.0 mM $CaCl_2$, 0.8 mM $MgSO_4$, 10 mM HEPES, pH 7.4).

Recording from Xenopus Oocytes—After incubation for 2–5 days, the oocytes were studied at room temperature (20–22 °C) in a 90-μl chamber. The oocytes were superfused with MBS at a rate of 6 ml/min. Agonists and chemical agents were diluted in the bathing solution and applied to the oocytes for a specified time, using a solenoid valve controlled superfusion system. Membrane currents were recorded by two-electrode voltage clamp at a holding potential of −70 mV, using a Gene Clamp 500 amplifier (Axon Instruments, Inc.). The recording microelectrodes were filled with 3 M KCl and had electrical resistances of 0.5–3.0 MΩ. Data were routinely recorded on a chart recorder (Gould 2300S). Average values are expressed as mean ± S.E.

Western Blot of Membrane Surface Receptor Proteins—*Xenopus* oocytes expressing 5-HT$_{3A}$ receptors were incubated with *N*-hydroxysuccinimide-SS-biotin (NHS-SS-biotin, Pierce) at a concentration of 1.5 mg/ml in PBS for 30 min at 4 °C under a nonpermeabilized condition, as described previously (18). The oocytes were then washed extensively and homogenized. The homogenate was centrifuged repeatedly at 1000 × *g* for 10 min at 4 °C until all yolk granules and melanosomes were pelleted. The final supernatant was incubated with 100 μl of NeutrAvidin-linked beads (Pierce) by end-over-end rotation for 2 h at 4 °C. The beads were centrifuged and washed extensively to isolate bead-bound proteins. Labeled proteins were eluted from the beads and loaded onto 10% SDS/PAGE. After transfer onto a polyvinylidene difluoride membrane (Invitrogen), the surface proteins were blocked with PBS (pH 7.5) containing 0.1% Tween-20 (Sigma) and 5% nonfat powdered milk and then incubated for 1 h with a polyclonal antibody (pAb120, 1:20,000) directed to the extracellular N-terminal domain of the 5-HT$_{3A}$ receptor (19). The proteins were washed, blotted with a 1:600 dilution of fluorescein-linked anti-rabbit IgG in PBS and incubated with anti-fluorescein AP conjugate (Pierce) at 1:2500 dilution in PBS for 1 h. The proteins detected by ECF substrate (Amersham Biosciences) were scanned using a Molecular Dynamics Storm Gel and Blot Imaging System with ImageQuant Image Analysis Software (Amersham Biosciences).

Cell Culture and Transfection—HEK293 cells obtained from the American Type Culture Collection were cultured in minimum essential medium supplemented with 10% heat-inactivated horse serum at 37 °C in 5% CO_2 and 95% air. Cells were plated at a density of 10^6 cells/ml in 35-mm dishes and allowed to grow to 70–95% confluence prior to transient transfection using calcium phosphate or Lipofectamine 2000 reagent (Invitrogen). The cDNA plasmid ratio for 5-HT$_{3A}$ subunits and green fluorescent protein (Invitrogen) was 3:1 (total amount of DNA: 4 μg).

Receptor Binding—HEK293 cells were incubated at 22 ± 1 °C for 60 min in various concentrations (10 nM) of [^{3}H]LY278,584 (specific activity = 64 Ci/mmol; Amersham Biosciences), a selective antagonist of 5-HT$_3$ receptor. The nonspecific binding was less than 5% of the total binding, as determined by incubation in 100 nM unlabeled LY278,584. The specific binding was determined by subtracting the nonspecific binding from the total binding. Each sample is the average from at least 3–4 separate experiments. Reactions were incubated for 1 h at 25 °C and were terminated by rapid vacuum filtration using a Brandel cell harvester onto GF/B filters followed by two rapid washes with 20 ml of ice-cold PBS buffer. Radioactivity was determined by scintillation counting. Data were analyzed by nonlinear sigmoidal dose-response curve fitting (PRISM).

Whole Cell Recording and Fast Solution Perfusion—Whole cell recordings were performed in HEK293 cells 1–3 days after transfection. HEK293 cells were re-plated on the day of the experiment. Cells were continuously superfused with a solution containing 140 mM NaCl, 5 mM KCl, 1.8 mM $CaCl_2$, 1.2 mM $MgCl_2$, 5 mM glucose, and 10 mM HEPES (pH 7.4 with NaOH, ~340 mOsm with sucrose). Membrane currents were recorded in the whole cell configuration using an Axopatch 200B amplifier (Axon Instrument) at 20–22 °C. Cells were held at −60 mV. Data were acquired using pClamp 9.0 software (Axon). Solutions were applied through two barrel theta glass tubing (TGC150, Warner Instrument) that had been pulled to a tip diameter of ~200 μm. The piezoelectric device was driven by

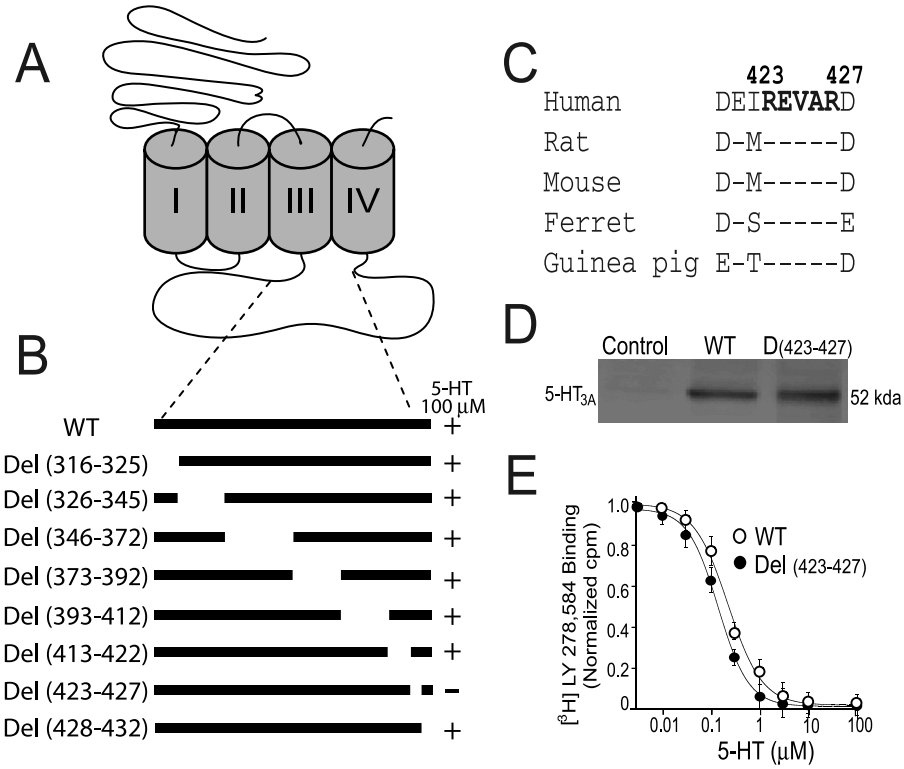

FIGURE 1. **Structural and functional analysis of the LCD of 5-HT$_{3A}$ receptor.** *A*, a topological model of the 5-HT$_{3A}$ receptor. The segment that was deleted in the LCD of 5-HT$_{3A}$ receptor is highlighted by a *dotted line*. *B*, schematic illustration of the sequential deletion of the segment in the LCD of the 5-HT$_{3A}$ receptor. The amino acid sequence shown is numbered following the deduced sequence of mouse 5-HT$_{3A}$ subunit, which contains a splicing variant of 6 amino acid residues in the cytoplasmic domain. The cRNAs of the mutant receptors were injected into *Xenopus* oocytes and the expression of these mutant receptors was determined using two-electrode voltage clamp after exposure to 100 μM 5-HT. *C*, the amino acid sequence within the 423–427 segment of the 5-HT$_{3A}$ receptor. *D*, Western blot of the membrane surface protein of 5-HT$_{3A}$ receptors expressed in *Xenopus* oocytes. *E*, ligand binding assay for the Del(423–427) mutant and WT 5-HT$_{3A}$ receptors. [^{3}H]LY-274,584 binding for the WT (*open circles*) and Del(423–427) (*solid circles*) receptors was carried out in HEK293 cells. The specific binding was determined by subtracting nonspecific binding (determined with 300 μM nonradiolabeled 5-HT). Each data point is the average from three individual binding experiments.

TTL pulses from the pClamp 9.0 software (Axon). Voltage applied to the piezo device produced a rapid lateral displacement (~50 μm) of the theta tubing to move the interface between control and test solutions. Solution exchange rate for open pipette and whole cell recording was estimated using the potential change induced by switching from the control solution to a 140 mM *N*-methyl-D-glucamine (NMDG) test solution at 0 mV in the absence of agonist; and the current rising phase was fit using an exponential function. The solution exchange time constants were ~0.3 ms for an open pipette tip and ~1.6 ms for whole cell recording.

Noise Analysis—Single channel conductances were determined using nonstationary variance analysis (20). Whole cell patch-clamp recording was performed at room temperature using an Axopatch 1D or 200B (Axon Instruments) amplifier. Patch-pipettes had tip resistances of 1–7 MΩ following fire polishing. Cells were voltage-clamped at −60 mV and were bathed in an extracellular medium containing (in mM): NaCl, 150; KCl, 5; $CaCl_2$, 0.2; HEPES, 10; glucose, 10; pH was adjusted to 7.4 using NaOH and osmolality to 340 mmol/kg using sucrose. Data were acquired at 5–10 kHz in 1s blocks on a computer using a DigiData interface and pClamp software (Axon Instruments). Records of current activated by 1 μM 5-HT were filtered (2 kHz 8-pole Bessel) and the DC component digitally subtracted. Variance of the AC component was determined and the background variance subtracted as described previously (20) and plotted against background-corrected mean current amplitude from the DC component. Unitary current was determined either from the slope of a least-squares linear fit to the data or from a fit of the data to the equation $\sigma^2 = iI - I^2/N$, where σ^2 is the current variance, i is the single channel current amplitude, I is the whole cell current amplitude, and N is the number of functional channels. Values for unitary current (in pA) were divided by the holding potential (in V) to yield single channel conductance (in pS).

Data Analysis—Statistical analysis of concentration-response data were performed with the use of the nonlinear curve-fitting program ALLFIT. Data were fitted using the logistic Equation 1,

$$Y = \{(E_{max} - E_{min})/[1 + (X/EC_{50})^n]\} + E_{min} \quad \text{(Eq. 1)}$$

where X and Y are concentration and response, respectively; E_{max} and E_{min} are the maximal and minimal responses, respectively; EC_{50} is the half-maximal concentration; and n is the slope factor (apparent Hill coefficient). Data were statistically compared by the paired Student's t test, or analysis of variance (ANOVA), as noted. Average values are expressed as mean ± S.E.

RESULTS

A Cytoplasmic Segment (423–427) Is Critical for Channel Gating—To understand the structural and functional role of the LCD in the 5-HT$_{3A}$ receptor (Fig. 1*A*), we sequentially deleted short regions of the LCD using the PCR technique (Fig. 1*A*). The LCD was first divided into 8 microdomains, each of which contains 5–25 amino acid residues (Fig. 1*B*). The cRNAs for the wild-type (WT) and mutant receptors were injected into *Xenopus* oocytes to determine the functional expression of these receptors. Most of these mutant receptors were functional when exposed to 100 μM 5-HT (Fig. 1*B*), except for Del(423–427), which resulted in a loss of function when expressed in both *Xenopus* oocytes and HEK293 cells. The amino acid sequence of this segment, Arg-Glu-Val-Ala-Arg, is highly conserved in the 5-HT$_{3A}$ receptors across different species (Fig. 1*C*). To determine

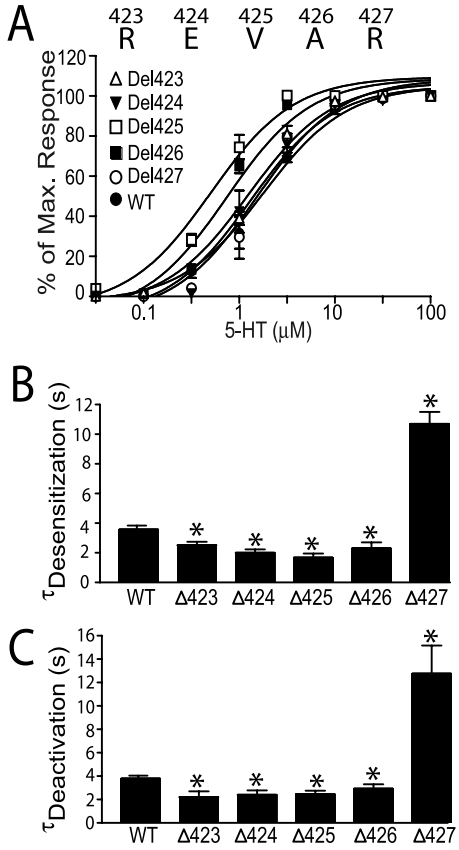

FIGURE 2. **Single amino acid deletions of the segment (423–427) alter receptor desensitization and deactivation.** *A*, the 5-HT concentration-response curves for the WT and mutant receptors. Graph plotting relative amplitude of 5-HT-activated current as a function of 5-HT concentration. Each data point represents the average current amplitude of 5–10 cells. *Error bars* not visible are smaller than the size of symbols. *B*, desensitization time constants of the WT and mutant receptors with sequential deletion of single amino acid residues within (423–427). *C*, deactivation time constants of the WT and mutant receptors. Note that deletion of Arg^{427} significantly slowed receptor desensitization and deactivation. *, $p < 0.01$, compared with WT.

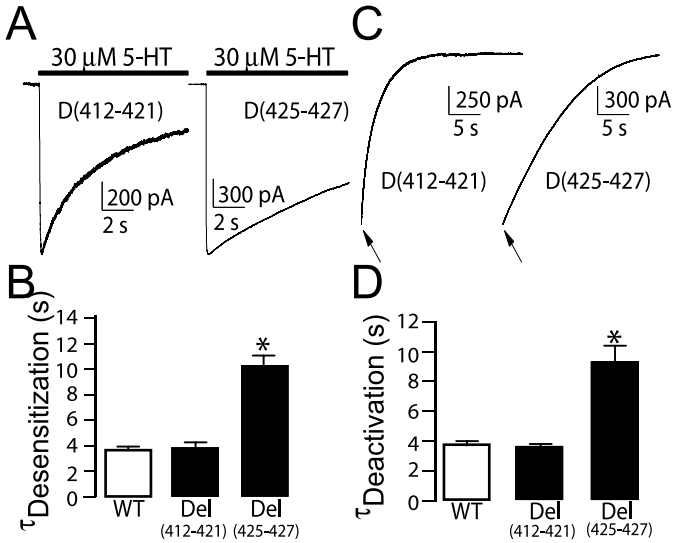

FIGURE 3. **Effects on receptor desensitization and deactivation by deletions of (412–421) and (423–427).** *A*, *traces* show desensitization in prolonged application of 30 μM 5-HT. The *solid bar* on top of each record indicates the time of agonist application. *B*, the *open bar* represents average desensitization time constant of the WT receptor. The *solid bars* (*from left*) represents average desensitization time constants of the mutant receptors with deletions of (412–421) and (425–427). *, $p < 0.01$, compared with WT. *C*, *traces* show deactivation kinetics following discontinuation of 1 mM 5-HT application. *D*, the *open bar* represents average deactivation time constant of the WT receptor. The *solid bars* (*from left*) represent average deactivation time constants of the mutant receptors with deletions of (412–421) and (425–427). *, $p < 0.01$, compared with WT.

whether or not Del(423–427) can affect the translational machinery and trafficking of the 5-HT$_{3A}$ receptor protein, we directly measured 5-HT$_{3A}$ receptor surface expression in oocytes by labeling cell surface proteins with sulfo-NHS-SS-biotin. A representative Western blot in Fig. 1*D* illustrates that the protein expression levels in the cell surface membrane did not differ between the WT and Del(423–427) mutant 5-HT$_{3A}$ receptors. To test whether the Del(423–427) mutant receptor retained 5-HT binding activity, we conducted ligand binding experiments in HEK293 cells transfected with the cDNAs for the WT and Del(423–427) 5-HT$_{3A}$ receptors. Fig. 1*E* illustrates the curves for displacement of specific binding of 10 nM [^{3}H]LY 278,584, a selective antagonist of 5-HT$_3$ receptors, by various concentrations of 5-HT in membranes isolated from cells transfected with the WT (*open circles*) and Del(423–427) mutant (*solid circles*) receptors. The values of K_d and the Hill coefficient were 0.25 ± 0.07 μM and 1.8 ± 0.1, respectively, for WT 5-HT$_{3A}$ receptors and 0.18 ± 0.03 μM and 1.6 ± 0.1 for the mutant receptors, respectively; these values are not significantly different (unpaired Student's *t* test, $p > 0.1$, $n = 12$).

Deletion of Single Amino Acid Residue at 427 Slows Receptor Desensitization—The above observations suggest that deletion of the entire segment (423–427) in the LCD of the 5-HT$_{3A}$ receptor can disrupt channel gating. To more carefully probe the structural and functional roles of individual amino acid residues within the segment (423–427), we sequentially deleted these residues one at each time. All of the point-mutated receptors were functional when expressed in both HEK293 cells and *Xenopus* oocytes. The maximal amplitude of 5-HT-activated current in cells expressing the mutant receptors did not significantly differ from that of the WT receptors (data not shown). In transfected HEK293 cell, deletion of Val^{425} or Ala^{426} significantly shifted in parallel the 5-HT concentration-response curves to the left of the WT receptor (Fig. 2*A*; $p < 0.01$, ANOVA and Tukey-Kramer test, $n = 5$), whereas deletion of Arg^{423}, Glu^{424}, or Arg^{427} did not significantly alter the 5-HT EC$_{50s}$ (Fig. 2*A*; $p > 0.2$, ANOVA and Tukey-Kramer test, $n = 5$–7). Next, we examined gating kinetics of the mutant receptors using fast perfusion. In HEK293 cells expressing WT 5-HT$_{3A}$ receptors, the average desensitization time constants of currents activated by 3, 30, and 1000 μM 5-HT were 6.1 ± 0.18 s, 3.8 ± 0.4 s, and 1.3 ± 0.02 s. These time constants are in agreement with results of previous studies (21–23). Deletion of Arg^{427} (Δ427) produced a marked slowing of desensitization and deactivation of the 5-HT$_{3A}$ receptors (Fig. 2, *B* and *C*, $p < 0.001$, ANOVA and Tukey-Kramer test, $n = 11$). In contrast, deletion of the other amino acid residues individually within the segment (423–427) accelerated the receptor desensitization and deactivation (Fig. 2, *B* and *C*, $p < 0.01$, ANOVA and Tukey-Kramer test, $n = 5$). All single amino acid deletions listed in Fig. 2 did not affect

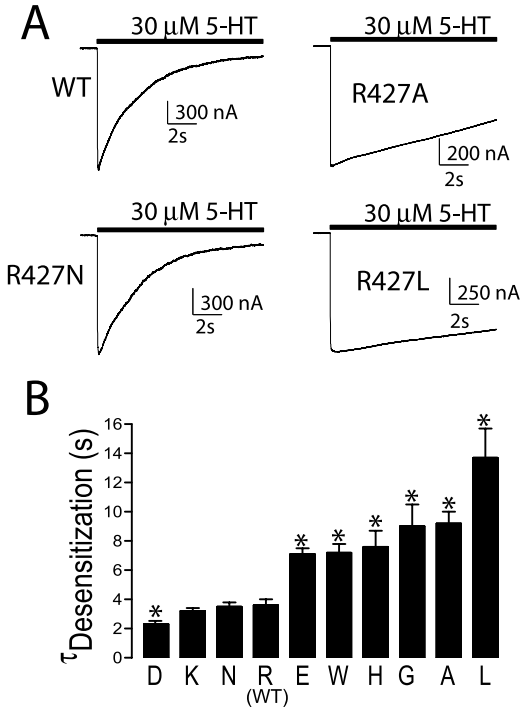

FIGURE 4. **Effects on receptor desensitization kinetics by multiple point mutations of the residue at 247.** *A*, traces show desensitization in prolonged application of 30 μM 5-HT. Note that the desensitization is slow in cells expressing the R427A and R427L mutants. The *solid bar* on top of each record indicates the time of agonist application. *B*, average desensitization time constants of the mutant and WT receptors. Each data point was determined from at least 5 cells. *, $p < 0.01$, compared with WT.

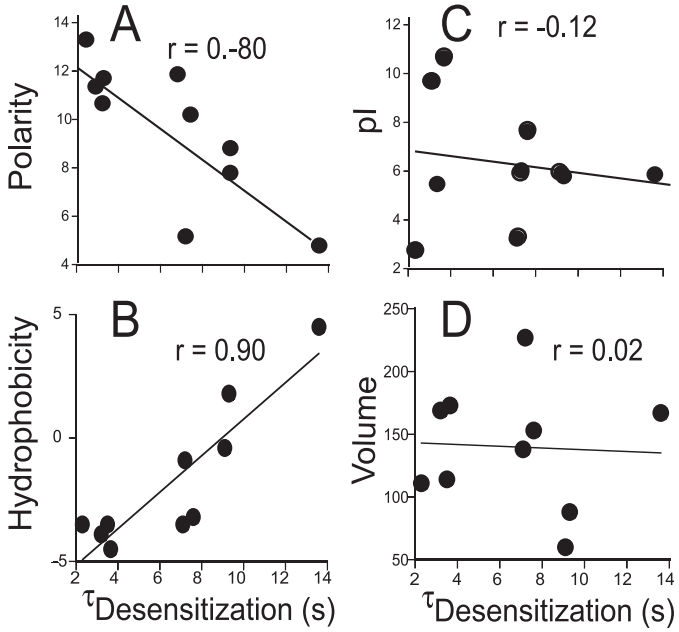

FIGURE 5. **Correlation analysis of the desensitization kinetics with properties of the amino acid residue at 427.** *A*, correlation of polarity of the amino acid residue at 427 with desensitization kinetics. *B*, correlation of hydrophobicity of the amino acid residue at 427 with desensitization kinetics. *C*, correlation of isoelectric point (pI) of the amino acid residue at 427 with desensitization kinetics. *D*, correlation of molecular volume of the amino acid residue at 427 with desensitization kinetics. Note that strong correlation was observed between the polarity and hydrophobicity of the residue at 427 with receptor desensitization.

5-HT$_{3A}$ receptor activation time constant (data not shown). To understand if Arg^{427} is a functionally dominant residue within the region (423–427), we deleted all three residues of 425–427 in one receptor. This deletion markedly slowed desensitization and deactivation of the 5-HT-activated current in a manner similar to that of the Arg^{427} deletion (Fig. 3, *A–D*). In contrast, deletion of an adjacent segment (412–422), which contains 10 amino acid residues, did not significantly affect the gating kinetics of the 5-HT$_{3A}$ receptor (Fig. 3, *A–D*; unpaired Student's *t* test, $p = 0.21$, $n = 5$).

The Extent of Receptor Desensitization Is Correlated with the Polarity of the Residue at 427—The above analysis revealed that deletion of a single amino acid residue at 427 can modulate desensitization kinetics in a manner similar to that produced by deletion of the whole (425–427) segment, suggesting that the residue at 427 may play a dominant role in regulation of receptor desensitization kinetics. To investigate the molecular basis of this regulation by Arg^{427}, we substituted the arginine at 427 with a series of amino acid residues and examined the desensitization kinetics of the mutant receptors. In general, replacing Arg^{427} with hydrophobic amino acid residues such as leucine (L) or alanine (A) substantially slowed the desensitization time constant of the 5-HT$_{3A}$ receptor, whereas replacing the Arg^{427} with polarized or hydrophilic residues such as lysine (K) or asparagine (N) accelerated receptor desensitization (Fig. 4, *A* and *B*). Next, we conducted linear regression analysis to compare the time constants of the desensitization kinetics with the biochemical and biophysical properties of the residue 427 including hydrophobicity (24), polarity (25), isoelectric point (pI) (from Lasergene, DNASTAR) and volume (26). Among these variables, the time constants for receptor desensitization were significantly linearly related to polarity and hydropathicity of the residue at 427 (Fig. 5, *A* and *B*, $p < 0.001$, linear regression analysis, $n = 10$). There was no significant relation between the desensitization time constants and the molecular volume and pI of the residue at 427 (Fig. 5, *C* and *D*, $p = 0.42$, linear regression analysis, $n = 10$). No such correlation was observed between the polarity of the residue 427 and the EC_{50} values for 5-HT (data not shown).

Effects of Point Mutations of Arg^{427} on the Single Channel Conductance of 5-HT$_{3A}$ Receptor—A previous study showed that point mutations of three arginine residues in the LCD of the human homomeric 5-HT$_{3A}$ receptors increased single channel conductance (27). One of the arginine residues (Arg^{440}) reported in this study is equivalent to the residue 427 of the mouse counterpart. In view of this, we conducted noise analysis experiments to examine the unitary conductance of the R427L mutant receptor, which exhibited the slowest desensitization kinetics. To get the largest possible conductance, we used a Mg^{2+}-free extracellular solution and with a relatively low concentration of Ca^{2+} (0.2 mM), because both divalent cations were found to reduce single channel conductance (20). The unitary conductance of the 5-HT$_{3A}$ receptor channels under these conditions was 1.3 ± 0.17 pS ($n = 5$) for the WT receptor (Fig. 6*A*), which agrees well with previous results obtained under similar conditions (20). In cells expressing the R427L mutant receptors, the unitary conductance was 1.1 ± 0.15 pS (Fig. 6*B*). These val-

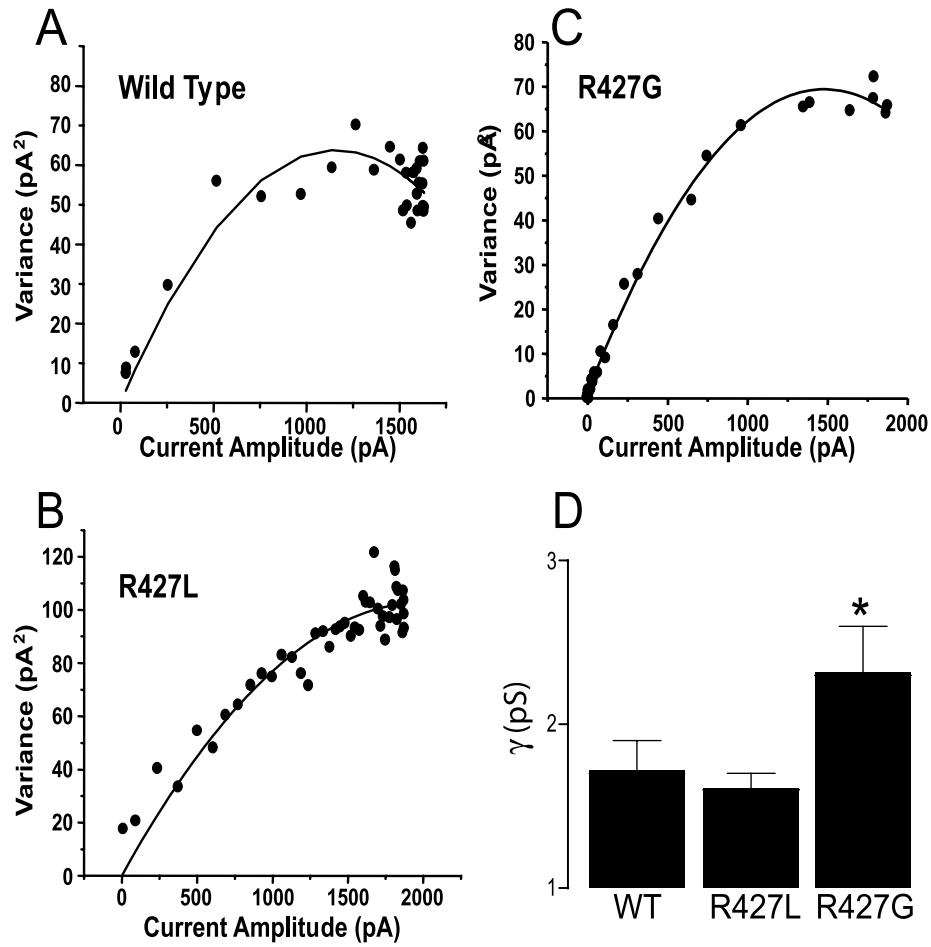

FIGURE 6. **Effect of point mutations at 427 on single channel conductance.** *A*, noise analysis of unitary single channel conductance of the WT receptors. Variance of the AC-coupled current in pA^2 is plotted against the DC current amplitude in pA. The curves shown are fits of the data to the equation given under "Materials and Methods." The values for estimated single channel conductance were obtained by dividing the estimated single channel amplitude from the fit (in pA) by the holding potential (−60 mV). *B*, in cells expressing the R427L mutant receptors, variance of the AC-coupled current in pA^2 is plotted against the DC current amplitude in pA. *C*, in cells expressing the R427G mutant receptors, variance of the AC-coupled current in pA^2 is plotted against the DC current amplitude in pA. *D*, *bar graph* represents average magnitude of single channel conductance measured by noise analysis. Each data point was determined from at least 5 cells. *, $p < 0.002$, compared with WT.

ues are not significantly different ($p = 0.44$, One-way ANOVA, $n = 5–8$). Note that the molecular volume of the alanine (A) residue that was used to place Arg^{427} residue (Arg^{440} of the human clone) is smaller than that of both leucine and arginine at 427. In this regard, we examined the unitary conductance of the R427G mutant and observed that the R427G mutation increased single channel conductance from 1.3 ± 0.2 to 2.3 ± 0.2 pS (Fig. 6*C*, $p < 0.002$, one-way ANOVA, $n = 5$).

In a separate study, we examined the current-voltage relationships of the WT and R427A mutant receptors with a voltage ramp from −80 to +60 mV at the peak of current activated by 3 μM 5-HT (Fig. 7*A*). The current evoked by 5-HT reversed at 1.1 ± 0.1 mV in the WT receptors and 1.3 ± 0.2 mV in the mutant receptors; these values are not significantly different ($p > 0.5$, unpaired Student's *t* test, $n = 5$). To further explore if the polarity of the Arg^{427} residue is conserved among the members of the Cys-loop LGIC superfamily, we aligned the amino acid sequence of the fragment that flanks Arg^{427} with equivalent sites in 13 other human receptors that belong to the LGIC superfamily (Fig. 7*B*). The residue corresponding to Arg^{247} in each receptor is highlighted in bold and italic. As can be seen, the polarity of Arg^{427} is indeed conserved across all of these subunits.

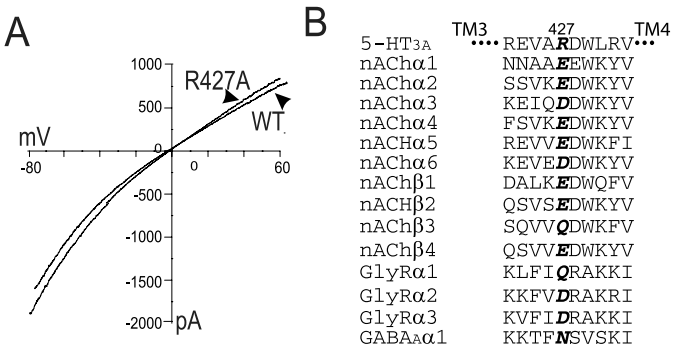

FIGURE 7. **The effect of the R427A mutation on reversal potential.** *A*, current-voltage relationships for the WT and the R427A mutant receptors. Each data point represents the mean ± S.E. from six cells. *B*, sequence alignment of the residue at 427. Amino acid sequence alignment of the Arg^{427}-containing segment across different subunits of human ligand-gated ion channels. Residues corresponding to Arg^{427} of 5-HT$_{3A}$ receptor are highlighted in *bold* and *italic*. Note that the hydrophilic nature of Arg^{427} is highly consistent among the members of the LGIC superfamily. The alignment was performed using Megalign of LaserGene program.

DISCUSSION

In the studies reported here, we have shown that deletion or point mutations of a single amino acid residue at position 427 of the 5-HT$_{3A}$ receptor slowed apparent desensitization without changing receptor activation kinetics. Such modulation appeared to be specific for the amino acid residue at 427, because deletions of the adjacent amino acid residues of the 5-HT$_{3A}$ receptor did not produce a similar effect on the desensitization kinetics. In addition, point mutations of Arg^{427} did not affect other channel properties such as single channel conductance and ion selectivity, indicating that a site at 427 in the large cytoplasmic loop of the 5-HT$_{3A}$ receptor is specific for regulation of desensitization kinetics.

Deletion of the segment 423–427 in the LCD of the 5-HT$_{3A}$ receptor resulted in a loss of channel function, as revealed by electrophysiological recordings. This was likely caused by

occlusion of channel gating rather than agonist binding, because both receptor protein expression at the cell membrane surface and receptor binding were unaffected by the 423–427 deletion. These findings suggest that this segment, which contains five highly conserved amino acid residues, is a structural element critical for channel opening. This notion is consistent with a previous prediction that a cytoplasmic domain containing arginine 423 and 427 residues of the 5-HT$_{3A}$ receptor participates in the formation of the intracellular portal of the channel pore (27).

The desensitized state of a receptor is proposed to have a higher affinity for agonist than that of the non-desensitized closed state (28). Accordingly, increases in desensitization rate can increase apparent agonist affinity (7, 8). In the present study, mutations at position Arg^{427} that decreased the rate of desensitization in the 5-HT$_{3A}$ receptor produced little or no change in the receptor sensitivity to agonist as assessed by 5-HT EC$_{50}$ values. The 5-HT EC$_{50}$ values of the WT and mutant receptors are not correlated with the extent of receptor desensitization. Thus, although increases in desensitization rate can increase apparent affinity, the present results are consistent with the view that desensitization has little influence on peak EC$_{50}$ value in the WT receptor. One of the possible mechanisms that may explain the kinetic changes by point mutations at Arg^{427} is that this mutation may increase the probability of the channel of being open, which could slow the time constant of desensitization. Unfortunately, investigation of this mechanism at the single channel level is not possible because of the low conductance of the homomeric channel (5). The slowing deactivation induced by the mutations of Arg^{427} could be caused by the receptor's stay in the open state being prolonged, because the open channel has been shown to lock the agonist from unbinding (29). It should be noted that we cannot rule out the possibility that the measurement of macroscopic receptor deactivation is, in fact, contaminated with receptor desensitization.

Our observation that measures of amino acid polarity were related to receptor desensitization may indicate that a hydrogen bonding-like interaction involving Arg^{427} may occur, which is involved in receptor conformational transitions conferring fast desensitization kinetics. On the other hand, increasing the hydrophobicity of the residue at 427 slowed this rate. The fast gating kinetics of the receptor implies that the free energy barrier required to switch between the closed and open states of the channel is relative low. Increasing the strength of a hydrophobic interaction at this position may be sufficient to tip the balance and bias the channel toward opening. It should be also pointed out that residues located in both sides of the membrane may collectively influence receptor gating kinetics (23), so that the overall ion channel gating kinetics likely reflects the coordinated influence of multiple sites throughout the protein.

Recent studies have shown that several key arginine residues including Arg^{423} and Arg^{427} within the LCDs of 5-HT$_{3A}$ and $\alpha4\beta2$ nACh receptors may serve as a common determinant of single channel conductance (17, 27, 30). Substitution of the arginine residues at 423 and 427 with aspartic acid (D) and alanine (A) residues resulted in increasing single channel conductance (17, 27, 30). These observations bring us a question on the structural and functional role of the very same amino acid residue at 427 in both receptor desensitization and single channel conductance events. Our observations reported in this study suggest that the molecular processes of receptor desensitization and channel conductance involving Arg^{427} should be mediated by distinct molecular processes. Consistent with this hypothesis, we observed that the R427L mutation significantly slowed desensitization kinetics without altering single channel conductance. In contrast, the R427G mutation slowed receptor desensitization and increased single channel conductance. This suggests that molecular basis involving Arg^{427} that modulates single channel conductance and desensitization kinetics may depend on the specific biochemical nature of the residue at 427. For instance, the extent of receptor desensitization is strongly correlated with the polarity of the residue at 427, whereas the single channel conductance is likely to be dependent on the molecular volume of the residue at 427: with reducing or increasing the molecular volume of the 427 residue, the single channel conductance varies. If this is the case, one should not expect any appreciable change in single channel conductance by a leucine (L) substitution of an arginine at 427 of the WT receptor, as the molecular volume of both residues is nearly identical. Moreover, we also observed that the receptor desensitization kinetics was not affected by deletion of Arg^{423}, which has been shown to be a critical site for single channel conductance (17). This also suggests that channel properties such as single channel conductance and desensitization should differ in their molecular basis.

It is interesting to note that the Arg^{427}, which links transmembrane domains with intracellular vestibule, is in an ideal position to transduce protein conformational changes required for receptor desensitization in the presence of agonists. Consistent with this hypothesis, a recent study using 5-HT$_{3A}$ receptor with an insertion of enhanced green fluorescent protein (EGFP) into the receptor LCD has revealed conformation changes cross the transmembrane domains to the intracellular side of the 5-HT$_{3A}$ receptor (31). Because the changes of EGFP fluorescence intensity after agonist application were stable for several minutes, it is likely that such transitions represent dynamic conformational changes of 5-HT$_{3A}$ receptor protein from an agonist-bound open state to a desensitized state.

In summary, the study reported here provides evidence that an arginine residue at 427 of the 5-HT$_{3A}$ receptor is critical for receptor desensitization through an interaction with neighboring amino acid residues. Because the members of Cys-loop LGIC superfamily are highly conserved in their amino acid sequences, our observations provide a new avenue for future studies to look for desensitization mechanisms of the 5-HT$_{3A}$ receptor as well as other members of the LGIC superfamily.

Acknowledgments—We thank Drs. David Julius and Sarah C. Lummis for providing us with mouse 5-HT$_{3A}$ subunit cDNA and the specific antibody against mouse 5-HT$_{3A}$ receptor. We thank Dr. David Lovinger for comments. We also thank Edgar Moradel and Gou-Xiang Lou for technical assistance.

REFERENCES

1. Maricq, A. V., Peterson, A. S., Brake, A. J., Myers, R. M., and Julius, D. (1991) *Science* **254,** 432–437
2. Grant, K. A. (1995) *Drug Alcohol Depend.* **38,** 155–171
3. van Hooft, J. A., and Vijverberg, H. P. (2000) *Trends Neurosci.* **23,** 605–610
4. Reeves, D. C., and Lummis, S. C. (2002) *Mol. Membr. Biol.* **19,** 11–26
5. Davies, P. A., Pistis, M., Hanna, M. C., Peters, J. A., Lambert, J. J., Hales, T. G., and Kirkness, E. F. (1999) *Nature* **397,** 359–363
6. Morales, M., and Wang, S. D. (2002) *J. Neurosci.* **22,** 6732–6741
7. Jones, M. V., and Westbrook, G. L. (1995) *Neuron* **15,** 181–191
8. Jones, M. V., and Westbrook, G. L. (1996) *Trends Neurosci.* **19,** 96–101
9. Wang, H. L., Milone, M., Ohno, K., Shen, X. M., Tsujino, A., Batocchi, A. P., Tonali, P., Brengman, J., Engel, A. G., and Sine, S. M. (1999) *Nat. Neurosci.* **2,** 226–233
10. Brownlow, S., Webster, R., Croxen, R., Brydson, M., Neville, B., Lin, J. P., Vincent, A., Newsom-Davis, J., and Beeson, D. (2001) *J. Clin. Investig.* **108,** 125–130
11. Engel, A. G., Ohno, K., Shen, X. M., and Sine, S. M. (2003) *Ann. N. Y. Acad. Sci.* **998,** 138–160
12. Yakel, J. L., and Jackson, M. B. (1988) *Neuron* **1,** 615–621
13. Lobitz, N., Gisselmann, G., Hatt, H., and Wetzel, C. H. (2001) *Mol. Pharmacol.* **59,** 844–851
14. Swope, S. L., Moss, S. J., Raymond, L. A., and Huganir, R. L. (1999) *Adv. Second Messenger Phosphoprotein Res.* **33,** 49–78
15. Hapfelmeier, G., Tredt, C., Haseneder, R., Zieglgansberger, W., Eisensamer, B., Rupprecht, R., and Rammes, G. (2003) *Biophys. J.* **84,** 1720–1733
16. Corringer, P. J., Le Novere, N., and Changeux, J. P. (2000) *Annu. Rev. Pharmacol. Toxicol.* **40,** 431–458
17. Peters, J. A., Hales, T. G., and Lambert, J. J. (2005) *Trends Pharmacol. Sci.* **26,** 587–594
18. Sun, H., Hu, X. Q., Moradel, E. M., Weight, F. F., and Zhang, L. (2003) *J. Biol. Chem.* **278,** 34150–34157
19. Spier, A. D., Wotherspoon, G., Nayak, S. V., Nichols, R. A., Priestley, J. V., and Lummis, S. C. (1999) *Brain Res. Mol. Brain Res.* **67,** 221–230
20. Brown, A. M., Hope, A. G., Lambert, J. J., and Peters, J. A. (1998) *J. Physiol.* **507,** 653–665
21. Gunthorpe, M. J., Peters, J. A., Gill, C. H., Lambert, J. J., and Lummis, S. C. (2000) *J. Physiol.* **522,** 187–198
22. Mott, D. D., Erreger, K., Banke, T. G., and Traynelis, S. F. (2001) *J. Physiol.* **535,** 427–443
23. Hu, X. Q., Zhang, L., Stewart, R. R., and Weight, F. F. (2003) *J. Biol. Chem.* **278,** 46583–46589
24. Kyte, J., and Doolittle, R. F. (1982) *J. Mol. Biol.* **157,** 105–132
25. Grantham, R. (1974) *Science* **185,** 862–864
26. Harpaz, Y., Gerstein, M., and Chothia, C. (1994) *Structure* **2,** 641–649
27. Kelley, S. P., Dunlop, J. I., Kirkness, E. F., Lambert, J. J., and Peters, J. A. (2003) *Nature* **424,** 321–324
28. Katz, B., and Thesleff, S. (1957) *J. Physiol.* **138,** 63–80
29. Chang, Y., and Weiss, D. S. (1999) *Nat. Neurosci.* **2,** 219–225
30. Hales, T. G., Dunlop, J. I., Deeb, T. Z., Carland, J. E., Kelley, S. P., Lambert, J. J., and Peters, J. A. (2006) *J. Biol. Chem.* **281,** 8062–8071
31. Ilegems, E., Pick, H., Deluz, C., Kellenberger, S., and Vogel, H. (2005) *Chembiochem.* **6,** 2180–2185